Penn Libraries
UNIVERSITY of PENNSYLVANIA

University of Pennsylvania
ScholarlyCommons

Departmental Papers (ESE)

Department of Electrical & Systems Engineering

April 2007

Fabrication of a Dual-Tier Thin Film Micro Polarization Array

Viktor Gruev
University of Pennsylvania

Alessandro Ortu
University of Pennsylvania

Nathan Lazarus
University of Pennsylvania

Jan Van der Spiegel
University of Pennsylvania, jan@seas.upenn.edu

Nader Engheta
University of Pennsylvania, engheta@seas.upenn.edu

Follow this and additional works at: http://repository.upenn.edu/ese_papers

Recommended Citation

Fabrication of a Dual-Tier Thin Film Micro Polarization Array

Abstract

A thin film polarization filter has been patterned and etched using reactive ion etching (RIE) in order to create 8 by 8 microns square periodic structures. The micropolarization filters retain the original extinction ratios of the unpatterned thin film. The measured extinction ratios on the micropolarization filters are ~1000 in the blue and green visible spectrum and ~100 in the red spectrum. Various gas combinations for RIE have been explored in order to determine the right concentration mix of CF_4 and O_2 that gives optimum etching rate, in terms of speed and under-etching. Theoretical explanation for the optimum etching rate has also been presented. In addition, anisotropic etching with 1μm under cutting of a 10μm thick film has been achieved. Experimental results for the patterned structures under polarized light are presented. The array of micropolarizers will be deposited on top of a custom made CMOS imaging sensor in order to compute the first three Stokes parameters in real time.

Comments

Fabrication of a Dual-Tier Thin Film Micro Polarization Array

Viktor Gruev, Alessandro Ortu, Nathan Lazarus, Jan Van der Spiegel and Nader Engheta

Electrical and Systems Engineering Department
University of Pennsylvania
Philadelphia, PA USA
vgruev@seas.upenn.edu

Abstract: A thin film polarization filter has been patterned and etched using reactive ion etching (RIE) in order to create 8 by 8 microns square periodic structures. The micro polarization filters retain the original extinction ratios of the unpatterned thin film. The measured extinction ratios on the micro polarization filters are ~1000 in the blue and green visible spectrum and ~100 in the red spectrum. Various gas combinations for RIE have been explored in order to determine the right concentration mix of CF_4 and O_2 that gives optimum etching rate, in terms of speed and under-etching. Theoretical explanation for the optimum etching rate has also been presented. In addition, anisotropic etching with 1μm under cutting of a 10μm thick film has been achieved. Experimental results for the patterned structures under polarized light are presented. The array of micro polarizers will be deposited on top of a custom made CMOS imaging sensor in order to compute the first three Stokes parameters in real time.

OCIS codes: (**120.5410**) Polarimetry. (**230.5440**) Polarization-sensitive devices. (**110.5220**) Photolithography.

References and Links

1. M.Born and E.Wolf, *Principles in Optics* (Pergamon, New York 1965).
2. Thomas W.Cronin and Justin Marshall, "Parallel Processing and Image Analysis in the Eyes of Mantis Shrimps," The Biological Bulletin **200,** 177-189 (2001).
3. T.Labhart, "Polarization opponent interneurons in the insect visual system," Nature **331,** 435-437 (1988).
4. A. G. Andreou and Z. K. Kalayjian, "Polarization imaging: principles and integrated polarimeters," IEEE Sensors Journal **2,** 566-576 (2002).
5. M. Momeni and A. H. Titus, "An analog VLSI chip emulating polarization vision of octopus retina," Neural Networks, IEEE Transactions on **17,** 222-232 (2006).
6. L. B. Wolff, T. A. Mancini, P. Pouliquen, and A. G. Andreou, "Liquid crystal polarization camera," Robotics and Automation, IEEE Transactions on **13,** 195-203 (1997).
7. J.S.Tyo, E.N.Pugh Jr., and N.Engheta, "Colorimetric Representations for Use with Polarization-Difference Imaging of Objects in Scattering Media," Journal of Optical Society of America A **15,** 367-374 (1998).
8. J.Guo and D.Brady, "Fabrication of high-resolution micropolarizer array," Optical Engineering **36,** 2268-2271 (1997).
9. J.Guo and D.Brady, "Fabrication of thin-film micropolarizer arrays for visible imaging polarimetry," Applied Optics **39,** 1486-1492 (2000).
10. Dennis Goldstein, *Polarized Light* (Marcel Dekker, New York ,NY 2003).
11. V. Gruev and R. Etienne-Cummings, "Implementation of steerable spatiotemporal image filters on the focal plane," Circuits and Systems II: Analog and Digital Signal Processing, IEEE Transactions on **49,** 233-244 (2002).
12. Gruev, V., J.Van der Spiegel, and N.Engheta. Image Sensor With Focal Plane Extraction of Polarimetric Information. 2006. IEEE ISCAS.
13. http://www.dymax.com
14. http://www.microchem.com
15. J.F.Battey, "Design criteria for uniform reaction rates in an oxygen plasma," IEEE Electron Devices 140-146 (1977).
16. J.M.Cook and B.W.Benson, "Application of EPR spectroscopy to oxidative removal of organic materials," Journal of Electrochemical Society **130,** 2459-2464 (1983).

17.   T.T.Wydeven, C.C.Johnson, M.A.Golub, M.S.Hsu, and N.R.Lerner. Plasma Polymerization. 299-314. 1979. Washington, D.C. ACS Symposium Series.
18.   http://www.edmundoptics.com

_____

1. Introduction

Polarization vision contains important information about the imaged environment, such as surface shapes, curvature and material properties, which are ignored with traditional imaging systems [1]. Several species of invertebrate, such as cuttlefish, mantis shrimp [2], desert ants and various other species of insects [3], rely on contrast enhancement using polarized vision, which is a vital survival mechanism in optically scattering media. The human eye perceives visual information in terms of color and intensity but it is essentially blind to polarization. Here, we are developing an imaging system capable of extracting almost the complete set of polarimetric properties for partially polarized light in parallel and real time. This sensory system integrates an array of imaging elements, a micro-polarization array and analog processing circuitry for polarimetric computation at the focal plane in order to achieve a compact, low power polarization sensitive system.

Biologically inspired, polarization difference (contrast) imaging (PDI) sensors have been one of the dominant research topics in developing polarization sensitive systems [4-6]. Several imaging systems have been made where polarization-contrast information has been computed at the focal plane [4,5] or with bulky, power hungry set-ups composed of CMOS/CCD imaging sensors, electro/mechanically controlled polarization filters and DSPs/CPUs [6,7]. These systems sample the environment via two orthogonal polarization filters and compute contrast information at the focal plane with translinear circuits or in the digital domain with a DSP/CPU. The sampling of the environment is achieved with spatially distributed polarization orthogonal filters over the neighborhood of two pixels or by temporally sampling the scene with two sequential orthogonal filters. Tradeoffs between these two approaches are reduction of spatial resolution in the former vs. reduction of frame rate in the latter system.

Incorporating pixel-pitch-matched polarization filters at the focal plane has been first reported by Andreou et al. [4], where birefringent materials and thin film polarizers have been explored. The pixel pitch for the birefringent and thin film micro-polarizer arrays was 50μm and 25μm, respectively. The large pixel pitch was limited by the wet isotropic etching technique employed for patterning the thin-film polarization filter and by the in-pixel circuit processing for extracting polarization contrast information in the birefringence imaging system. An 8 by 5 birefringent micro-polarization element array with pixel-pitch size of 128μm was reported in [5]. The large pixel pitch in these polarimetric imaging systems limits the fidelity of the imaged environment, which is a major shortcoming for high resolution imaging applications.

Another avenue of research has been the design of micro-polarization array for extracting the complete set of polarimetric properties of partially linearly polarized light. A micro-polarization array with three spatially distributed polarizers was fabricated and described by Guo et al. [8]. The polymer thin film was used to create a three axial micro polarizer array with 25 micron pixel pitch elements. A dual axel dichroic-on-threated-glass micro polarizer array with 5μm pixel pitch and extinction ratio of ~330 was reported in [9].

The previously reported PDI systems, which have been directly inspired from biological systems, compute polarimetric information in simplified and compact form [4,5]. In contrast, the complete polarimetric information tends to be far more complex and its computational demands usually prevent real time extraction [10]. These complex polarization properties are fully described by the four fundamental parameters known as the Stokes parameters. For natural lights, which are usually polychromatic and partially polarized and for which the phase information between the components is not available, only the first three Stokes

parameters are needed. In order to fully determine these three Stokes parameters, the imaged scene must be sampled at least with three different polarization filters.

We are developing a high resolution imaging system capable of extracting the first three of the four Stokes parameters from the imaged environment in parallel and in real time. This novel sensory system integrates imaging array with 10μm pixel pitch with a photodiode area of 8x8 μm square, pitch-matched-micro polarization array and polarization processing at the focal plane.

In this paper we solely focus on the microfabrication steps necessary for patterning a commercially available thin film polarizer in order to create a dual axel micropolarization array with 8μm by 8μm square filters. The paper is organized as follows. In Section 2, a theoretical background on light polarization is presented in order to introduce a technique for polarimetric computation at the focal plane. Section 3 presents the micro fabrication steps necessary to manipulate thin film polarizer. RIE effects on the polarizer are theoretically analyzed in Section 4. Experimental data is presented in Section 5 and concluding remarks are summarized in Section 6.

2. Overview of polarization information and Stokes parameters

Stokes parameters can describe the polarization information of light. There are different ways to express Stokes parameters, one of which is presented by equations (1) through (4), which describe fully the polarization state of the electric-field vector.

$$S_0 = I_t \tag{1}$$

$$S_1 = 2I(0^\circ, 0) - I_t \tag{2}$$

$$S_2 = 2I(45^\circ, 0) - I_t \tag{3}$$

$$S_3 = I_t - 2I(45^\circ, \pi/2) \tag{4}$$

In equations (1) through (4), I_t is the total intensity; $I(0^0,0)$ is the intensity of the e-vector filtered with a 0 degree polarizer and no phase compensation between the x and y components; $I(45^0,0)$ is the intensity of the e-vector filtered with a 45 degree polarizer and no phase compensation as above; and $I(45^0,\pi/2)$ is the intensity of the e-vector filtered with a 45 degree polarizer and $\pi/2$ phase compensator between the x and y components. The first three Stokes parameters fully describe the polarization of light with two linearly polarized intensities and the total intensity of the e-field vector. Therefore, in order to fully describe the polarization state of light in nature, for which the phase information between the components is not available, three linearly polarized projections or two linearly polarized projections in combination with the total intensity are needed. The latter method is preferred for focal plane implementation since it only requires two thin film polarizers offset by 45 degrees, patterned and placed on neighboring pixels. The overall thickness of the complete filter will be thinner for a two-tier vs. a three tier filter, which has two main advantages. The first advantage is in minimizing light attenuation through multiple layers and increasing the angle of incidence. The second advantage is in reduction of fabrication steps and minimization of alignment errors.

The patterning of the thin film polarizer is similar to the Bayer pattern used in color imaging and it is shown in Figure 1 together with the image sensor. The image sensor is composed of an array of 256 by 256 photo pixels, and the noise suppression and analog computation circuitry is included at the focal plane. The micropolarizer array is separately attached on the image sensor with the pattern shown in Figure 1.
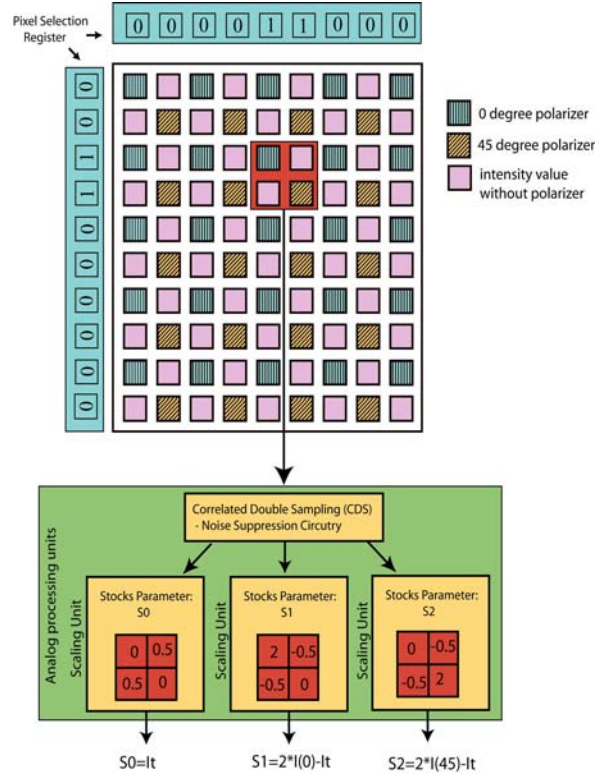
Figure 1: Block diagram of the complete imaging system: imaging array, processing circuitry and micropolarization array

In the image sensor presented in Figure 1, a neighborhood of 2 by 2 pixels is addressed and accessed simultaneously. In the pixels neighborhood of interest, one pixel records the 0 degree projected polarized image ($I(0^0,0)$), another records the 45 degree projected polarized image ($I(45^0,0)$) and two pixels record the unfiltered intensity image (I_t). The polarimetric parameters are estimated by reading out all four pixels in parallel [11] and scaling them individually at the periphery, i.e. away form the imaging array, with programmable analog scaling circuitry in accordance to the first three Stokes parameter equations (equation (1) through (3)). The details of the addressing scheme of block of 2 by 2 pixels and analog processing circuitry are described in [12].

3. Micro fabrication steps for thin film polarizer manipulation

A commercially available thin film polarizer is used to create an array of micropolarizers. The thin film polarizer consists of an iodine-doped Polyvinyl Alcohol (PVA) layer, which acts as a dense array of thin microscopic wires. These microscopic wires are formed by mechanically stretching the polymer film, allowing the molecules of the PVA to align in the direction of stretching. In order to have an effective polarizer, the size and spacing between the thin microscopic wires should be ~1/100th and ~1/10th of the light's wavelength, respectively [10]. For example, for blue light wavelengths or 450nm wavelength, the distance between the microscopic wires should be on the order of 45nm, while the thickness of the wires should be around 5nm. The mechanical stretching of the polymer creates a very good ~10μm thick polarization filter for the visible spectrum, with extinction ratios of about 1000 in the blue and green spectrum and 100 in the red spectrum. The PVA thin film is placed between two 300μm thick transparent Cellulose Acetate Butyrate (CAB) or polyethylene layers (Figure 2-a). The CAB layers provide structural stability to the fragile and thin PVA layer.

In order to be able to manipulate the PVA layer, at least one of the protective CAB layers must be removed. Since CAB is a form of acetate, it is therefore acetone soluble. Hence, the sample is submerged in an acetone bath for 30 minutes. One side of the sample is taped with an acetone resistant tape, i.e. rubber tape, to a glass substrate in order to protect the bottom layer of CAB which provides structural stability for the PVA layer. The sample is rinsed with de-ionized water (DI) in order to remove the soften CAB layer. The DI water also solidifies the CAB layer, upon which the sample is submerged in the acetone bath again. These two steps are repeated several times, until no residual CAB layer remains on top of the PVA layer (Figure 2-b).

The next step is to glue the PVA to a substrate. In the final imaging system, the PVA will be glued directly to the die of the imaging system. For testing purposes, however, the PVA is glued to a microscopic glass in order to be able to back illuminate the filter and to fully characterize the optical properties of the micro-polarizer elements. A UV sensitive adhesive promoter, Dymax AD420 [13], is used between the PVA and the IC/Glass substrate (Figure 2-c). The UV adhesion promoter has 95% transparency, which allows for minimal absorption of the impingent light wave. The adhesive promoter exhibits minimum expansion when heated and it has an important property for preserving the extinction properties of the PVA layer.

The next step is to remove the bottom CAB layer in order to allow patterning the PVA film. This step is similar to the initial step, where a repeated acetone bath and DI water rinsing are used. The final structure after this process is shown in Figure 2-d.

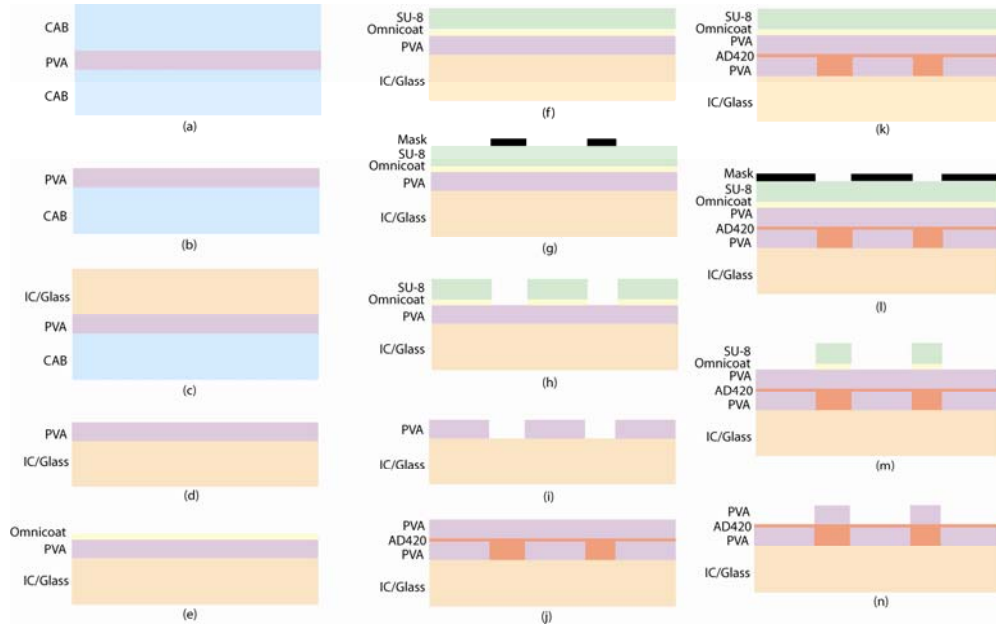The remaining steps describe the patterning and etching process of the PVA. These steps are as follow:

Figure 2: Microfabrication steps for creating a dual layer polarization structures

(1) Heat the sample to a temperature of 95°C for 5 minutes. This ensures that the surface of the PVA is completely dry. An adhesion promoter, Omnicoat [14], is applied directly and spin coated at 3000 rpm for 60 seconds. The sample is then baked for 1 minute at 95°C. The Omnicoat layer promotes adhesion between the PVA and the SU-8 photoresist (Figure 2-e).

(2) Immediately apply an SU-8 2015 negative photoresist [14] on top of the PVA. The negative photoresist, SU-8 2015, is hydrophobic and requires the surface of the PVA to be absolutely free of any water molecules. If the sample is cooled down to room temperature,

water molecules due to humidity will coat the surface of the PVA. The adhesion of the SU-8 will be virtually non existent when patterning 10μm or smaller structures. Larger structures tend not to have problems with adhesion when the PVA is cooled down to room temperature.

(3)   Spin coat the photoresist at 500rpm for 10 seconds and then at 3000 rpm for 50 seconds with 500 rpm per second acceleration. The resulting photoresist thickness is 3μm.

(4)   Bake the sample at 65^OC for 1min and then at 95^OC for 2min. It is recommended that the sample cools down at 65^OC for 1 min in order to gradually decrease the temperature of the sample. Gradual increase and decrease of the temperature during the baking process avoids rapid temperature differences and prevents the photoresist from cracking (Figure 2-f).

(5)   Expose the photoresist at 375nm wavelength for 20 seconds at 8mW/cm^2 intensity. The mask used to pattern features for the imaging sensor contains 10 μm by 10 μm square patterns (Figure 2-g). This mask allowed us to closely evaluate isotropic etching properties using an electron scanning microscope.

(6)   Post-bake the sample at 65^OC for 1 min and then at 95^OC for 2 min. The sample is cooled down at 65^OC for 1 min in order to gradually decrease the temperature and minimize stress and cracking on the photoresist.

(7)   Develop the photoresist for 4 min in an SU-8 developer and gently rinse it with isopropyl alcohol. If white colored liquid appears on the surface, the photoresist is not completely developed and it is submerged in the developer again (Figure 2-h).

(8)   Selective reactive ion etching is performed on the sample. A mixture of gasses composed of 28 sccm Ar, 30 sccm O_2 and 10 sccm CF_4 is used. The RF power is 150W, at 17^OC temperature and 20mbar pressure. The selected ratio of the appropriate gasses is optimized to maximize the etching of the PVA while minimizing the destructive etching of the SU-8 photo resist. The etching rate of the PVA is 0.5μm/min, while the etching rate of the SU-8 is 0.75μm/min. Since the thickness of the PVA is ~10μm, the sample is etched for ~20 minutes. The thickness of the SU-8 is optimized to be 15μm and it will be etched completely by the time the PVA layer is etched. This optimization simplifies the microfabrication procedure at the cost of slightly damaging the PVA structures which might occur due to variations in the PVA and SU-8 thickness.

A more conservative approach can be employed, where the SU-8 thickness can be increased above 15μm. Once the etching of the PVA layer is completed, the remaining photoresist can be removed with an SU-8 photoresist striper. The Omnicoat layer helps lift the SU-8 photoresist and remove it from the PVA structures. The RIE provided anisotropic etching with ~1μm under cutting, compared to 4μm and 10μm under cutting with oxygen plasma and wet etching, respectively (Figure 2-i).

The next step is to add a second layer of PVA on top of the first layer offset by 45 degrees via a UV adhesive promoter and etch it with the desired mask pattern. Following the adhesion procedure, the top CAB layer is removed with acetone in order to be able to pattern the PVA layer. This step is similar to the initial step, where a repeated acetone bath and DI water rinse is used. The final structure after this process is shown in Figure 2-j. The remaining steps for patterning the top layer of PVA are identical to the one for patterning the bottom layers. These steps are shown in Figure 2-k through Figure 2-n. The final two-axial micro polarization filter is shown Figure 2-n, with a total thickness of around 20μm.

4.   Reactive Ion Etching (RIE) Effects on the PVA

Cold plasma or RIE has been widely used to modify or etch polymers. The etching process of polymers is linearly dependent on the concentration of the atomic-oxygen free radicals [15] or on the number of oxygen atoms consumed during the etching process [16]. Since the PVA is an unsaturated polymer, the etching process is represented as addition to unsaturated moieties [17]. The addition of oxygen to the unsaturated PVA creates a saturated radical with a weakened C-C bond. Any subsequent attack by free oxygen radicals will break the C-C bond and it will divide the saturated molecule. Carbon monoxide (CO) and carbon dioxide (CO_2) are released during the etching procedure (equation 5).

$$\begin{array}{c} \textbf{O-O} \\ | \\ \textbf{-C=C- + O}_2 \textbf{: -> -C-C- +O}_2 \textbf{-> -C=O +CO} \end{array} \qquad (5)$$
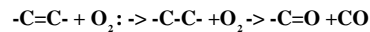
   In order to increase the etching rate of the PVA, the concentration of oxygen atoms must be increased. This is achieved with the addition of fluorine gases, such as CF_4, CF_3, C_2F_6, SF_6 and others. In our experiment, CF_4 was used. The enhanced etching rate is due to the increased density of electrons, as well as increased energy of electrons in the RIE. At the molecular level, the addition of fluorine atoms further weakens the C=C bond of the PVA molecule and it creates a saturated radical prone to chain scission. The fluorine gases combine with the carbon and oxygen atoms and create a fluorinated ethane and ethylene derivative. These stable fluorine products remain on the surface of the PVA. If the concentration of the fluorine atoms is increased beyond a threshold, fluorinated ethane will have retarding effects on the etching rate. The fluorinated ethane has to be removed before reaching the PVA surface and etching the PVA surface. Hence, the etching rate exhibits a maximum for a given concentration ratio of O_2 and CF_4 and it rapidly decreases with the increase or decrease of the CF_4 concentration.

   We have performed experiments where the concentration of CF_4 was varied in order to determine the optimum etching rate. From Figure 3, we can observe that for 30% of CF_4 in a total mixture of O_2 and CF_4, the PVA exhibits a maximum etching rate. Deviations from this optimal concentration have retarding effects on the etching rate as it is expected form the theory. Since the SU-8 photoresist is a polymer, it also exhibits similar etching behavior as the PVA. Due to its different molecular composition, the SU-8 has slightly higher etching rate then the PVA. This should be taken into account for the final thickness of the SU-8, as the SU-8 acts as protective layer for the PVA and it should remain until the unprotected PVA is etched completely. From the experimental data, an Oxygen-to-Freon (CF_4) ratio of 3:1 yields an optimum etching results. For this gases concentration, the etching rate of the SU-8 is 0.75µm/min, while the etching rate for the PVA is 0.5µm/min.
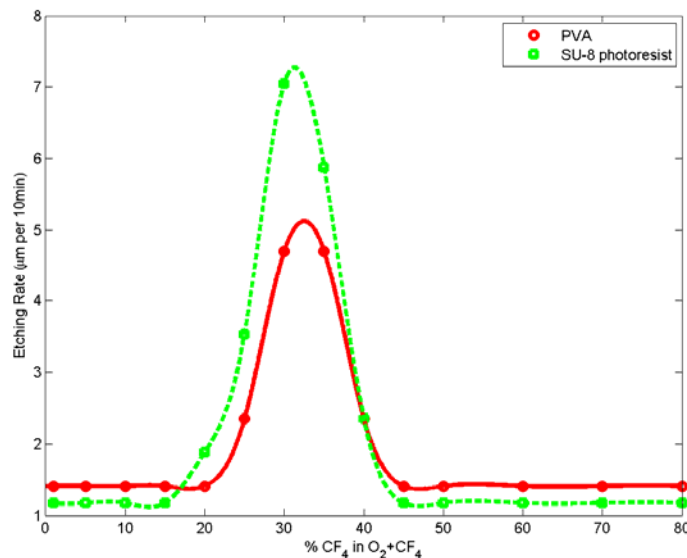

Figure 3: Etching rate of PVA and SU-8 as a function of a CF_4 concentration in an O_2 and CF_4 gas mix.

5. Dual-tier micro polarization array: Experimental results

The final two-tier micro polarization array was tested for its structural and optical properties. A scanning electron microscope (SEM) was used to evaluate the photoresist and the etched PVA structures. A comparison of the size of both structures indicated the amount of under-etching due to the selective RIE procedure.

In Figure 4-a and Figure 4-b, the SU-8 square structures obtained after the photolithography procedure (see Figure 2-h) are presented. Figure 4-a presents the photoresist structures viewed from the top, while Figure 4-b present an array of photoresist pillars recorded under 52 degree angle tilt. The photoresist squares are 10µm by 10µm wide and 15µm tall, with 10µm spacing between neighboring structures. The corners of the square structures are slightly rounded due to edge diffraction effects from the mask. The rounding effects are minimized by optimizing pre-baking, post-baking and exposure time of the photoresist. The uniform periodic structures are observed in Figure 4-b.

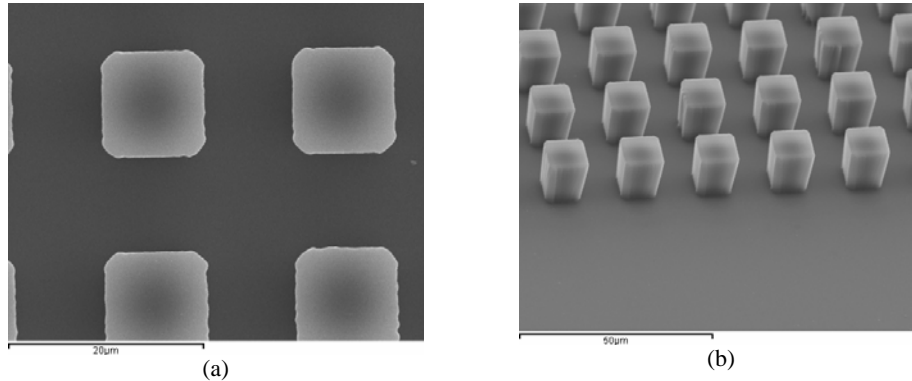(a)   (b)

Figure 4: Scanning electron microscope images of the developed SU-8 photoresist structures. Left panel shows a top view of a small neighborhood of SU-8 squares with 10µm by 10µm pitch. Right image shows an array of periodic SU-8 square structures with 15µm thickness, which was recorded under 52° angle tilt.

After the selective reactive ion etching of the top PVA layer (see Figure 2-n), the micro polarization structures were evaluated under an SEM. Figure 5-a and Figure 5-b present the top PVA layer of the complete two-tier filter. The left panel presents a top view of a small neighborhood of micropolarizer structures. The square PVA structures have 8µm by 8µm size with 12µm spacing between neighboring structures. Therefore, the undercutting due to the RIE is 1µm per side and the final size of the PVA square structures have decreased by 2µm from the original 10µm photoresist structures. Readjusting the size of the squares on the mask (i.e. photoresist structure) to 12µm will lead to 10µm PVA square structures. Since, our photo pixel has a fill factor of 64% (i.e. the photodiode area is 8µm by 8µm), the obtained size of the PVA structures satisfied the minimum size requirements.

The right image in Figure 5, which was recorded under 52 degree angle tilt, presents a single PVA micro structure of size 8µm by 8µm and 10µm thickness. The PVA structure does not contain any residual SU-8 photoresist since the thickness of the photoresist was optimized to be completely etched away during the selective RIE procedure. Furthermore, we can observe that the top of the PVA structure is not smooth, which indicates that it has been partly etched. This is a result of small variations in the PVA thickness as well as variations in the SU-8 photoresist. Hence, precise etching time for the PVA can not be determined. The top of the PVA structures was spin coated with an adhesive promoter AD420 since it has an index of refraction similar to the PVA (n=1.41). This prevented any undesirable diffraction which might occur at the surface of the PVA. Although the top portion of the PVA has been etched (around 0.3µm from the 10 µm total thickness), the optical measurements of the PVA

(a)

(b)
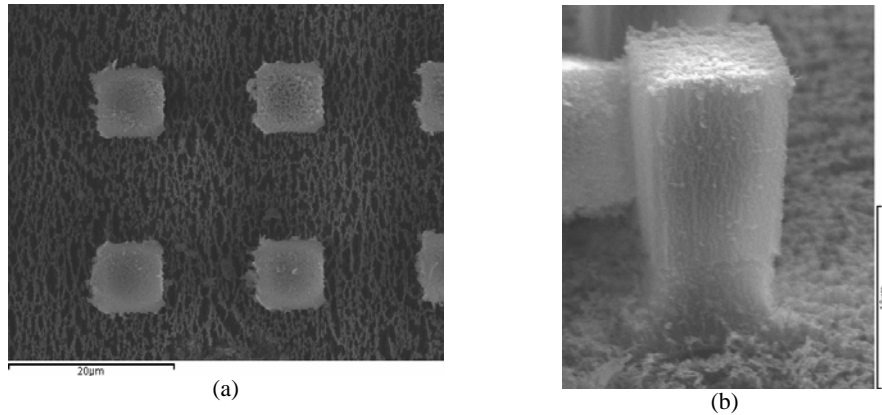
Figure 5: Scanning electron microscope images of the top PVA tier. Left image shows an array of 8μm by 8μm PVA structures. Right panel shows a single PVA structure with 8μm pitch and 10μm thickness, which was recorded under 52 degree angle tilt.

structures have shown that the extinction ratios have been preserved during the etching procedure.

The optical properties of the dual-tier micro polarization filter were evaluated under an optical microscope via back polarized illumination of the sample with three different wavelengths: 720nm wavelength (red light), 580nm wavelength (green light) and 480nm wavelength (blue light). We have created two samples of a dual-tier micro polarization filter. In the first sample the two layers of micropolarizers are offset by 90 degrees, while in the second sample they are offset by 45 degrees. The second sample contains the desired pattern which will be integrated with a CMOS image sensor in order to extract the first three Stokes parameters. The first sample was used for measurement purposes and for visual clarity, although it can be used for a polarization difference (contrast) computation [6,7].

The optical characteristics of the dual axial micropolarizers offset by 90 degrees are presented in Figure 6. In Figure 6-a, the sample was illuminated with polarized light having polarization perpendicular (parallel) to the transmission axis (axis of polarization) of the PVA structures in the first tier. The square structures in the first tier appear bright in intensity and little darker compared to the background since the PVA attenuates part of the parallel polarized light (PVA transmission of about 40% has been measured and reported in the literature [18]). The square structures in the second tier appear opaque. They attenuate the
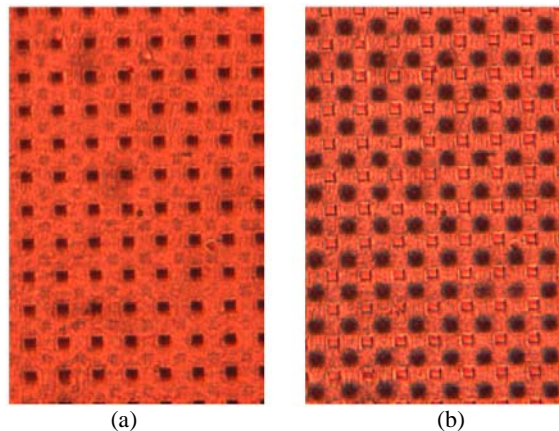

(a)

(b)

Figure 6: Experimental results for the dual-tier micro polarization filters offset by 90 degrees. The first layer in the left sample attenuates perpendicular polarized light while the second layer is transparent. The reverse is observed in the right sample.

intensity of the incoming light waves since their axis of polarization is oriented perpendicular to the polarization of the incident polarized light. In Figure 6-b the sample was illuminated with polarized light perpendicular (parallel) to the transmission axis (axis of polarization) of the PVA structures in the second tier. The reverse effects are observed in this image, where the top layer is opaque and the bottom layer is transparent due to the 90 degree polarization offset of the illuminating light source. Since the square structures in the dual axial filter reside in different tiers separated by 10µm and the images were taken under a microscope with 5 µm depth of focus, the contours of the square structures in the bottom tier appear slightly blurred. Refocusing the microscope to image the bottom tier structures verified the sharpness of the squarely-etched structures.

The optical characteristics of the dual-axial micropolarizers offset by 45 degrees are presented in Figure 7. The images in Figure 7-a, 7-b, 7-c and 7-d are recorded with 0, 45, 90 and 135 degrees of polarized light, respectively. In Figure 7-a (Figure 7-c), the sample was illuminated with polarized light with polarization parallel (perpendicular) to the transmission axis of the PVA structures in the first tier i.e. with 0 (90) degree polarized light. Hence, the square structures in the first tier appear opaque in intensity in Figure 7-a and transparent in Figure 7-c. Since the second tier is offset by 45 degrees, it is difficult to visualize its relative offset. The polarization properties of the second tier are clearly evident in Figure 7-b and Figure 7-d. In Figure 7-b (Figure 7-d), the sample was illuminated with polarized light parallel (perpendicular) to the transmission axis of the PVA structures in the second tier i.e. with 45 (135) degree polarized light. Hence, the square structures in the second tier appear opaque in intensity in Figure 7-b and transparent in Figure 7-d.
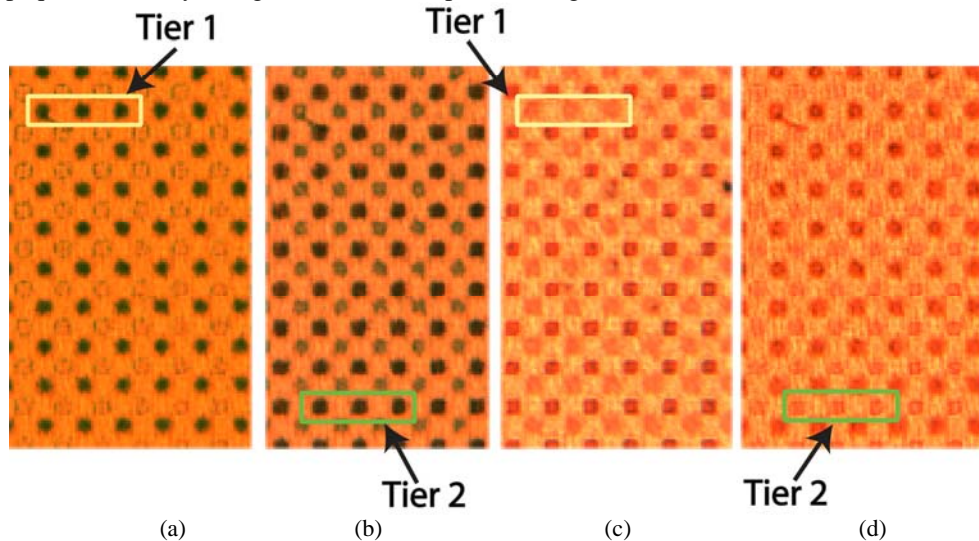

| (a) | (b) | (c) | (d) |

Figure 7: Experimental results for the two axial micro polarization filters offset by 45 degrees. The images are illuminated with 0, 45, 90 and 135 degree polarization for the incident polarized light, respectively.

Figure 8 and Figure 9 present movies, demonstrating the polarization filtering capabilities of the dual-tier and single-tier micro-structured PVA, respectively. The offset of the two-tier samples is 45 degrees. The movie files are composed of 36 frames, where the angle of polarization of the light source is varied between 0 degrees and 180 degrees in increments of 5 degrees between frames. The filter was illuminated with red-light wavelength in both examples; hence the transparent background of the sample appears red. The samples were illuminated with all three wavelengths separately in order to evaluate the dependence of the extinction ratios on the wavelength, but for the sake of brevity only one wavelength is presented here in the movie files. In Figure 8, it can be observed that initially the bottom layer is transparent and the top layer is opaque. As the angle of polarization is varied between
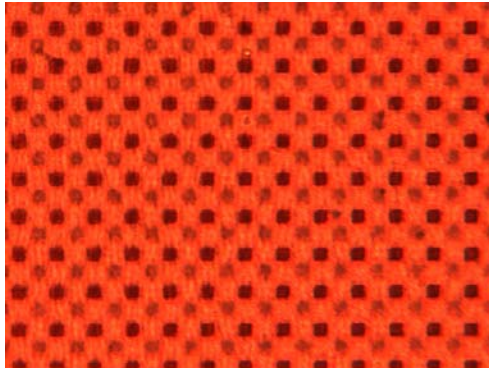
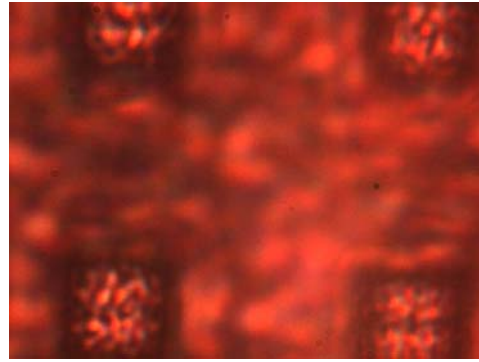Figure 8: (3 MB) Movie of the dual axial micro polarizer array (13MB version).

Figure 9: (3 MB) Movie of a single micro polarizer element (12MB version).

frames, the transparency shifts from the top PVA tier to the bottom PVA tier. Since the data was taken while focusing on the PVA structures on the top tier, the PVA structures in the bottom tier appear slightly blurred and unfocused. In Figure 9, we observe the polarization behavior of a single PVA tier. The PVA structure gradually changes from transparent to opaque as the angle of polarization is changed. In this figure, we can closely monitor that the effective size of the PVA structures is 8μm by 8μm, demonstrating anisotropic under-etching of 1μm during the RIE procedure.

The two-tier filter, where the tiers were offset by 90 degrees, was also recorded with a 12 bit grayscale camera. Since the extinction ratio of the un-patterned PVA is around 1000 [18], the sensitivity of the imaging devices has to be at least 10 bits or higher. Two regions of 10 by 10 pixels were selected in Figure 8, which corresponded to two PVA structures in separate tiers. The average intensity value was computed and normalized to the incident light intensity on the filter. The data was recorded over 36 frames, where the angle of polarization was incremented by 5 degrees between frames. The transmission properties of both tiers, presented in Figure 10, closely follow Malus' cosine low for polarization irradiance [1]. Since the two PVA layers were offset by 90 degrees, the maximum and minimum transmissions between the two-tiers are expectedly shifted by 90 degrees.
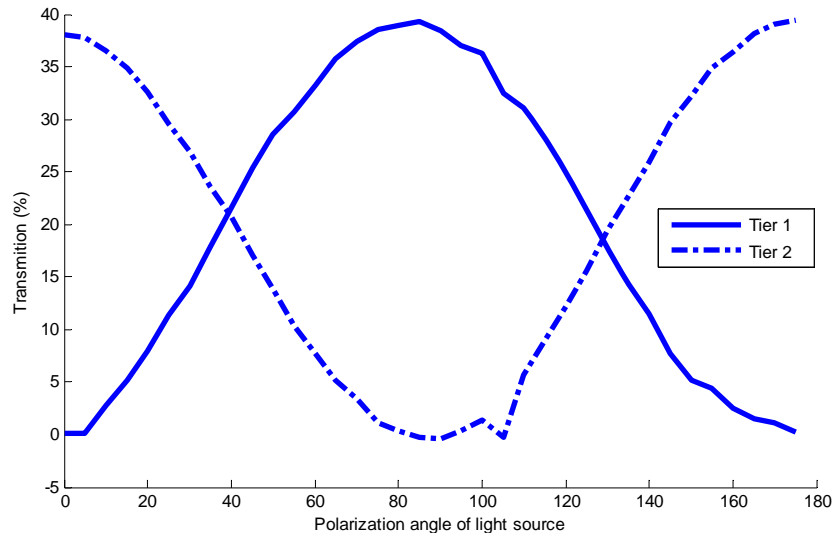

Figure 10: Transmission of both PVA structures follow Malus' law for polarization irradiance

The extinction ratios for the patterned PVA structures were also evaluated at three different wavelengths. Figure 11 presents the transmission percentage as a function of the angle of polarization for three different wavelengths. Also, transmission data for an unpatterned PVA sample was recorded and presented with black dotted line in Figure 11. From this data, the extinction ratios, defined as the ratio of the maximum to minimum transmission for a given wavelength, were calculated. The maximum transmissions for red and blue wavelength were recorded to be 45% and 40% respectively. The minimum transmissions for the red and blue wavelength were recorded to be 0.4% and 0.04% respectively. Therefore, the extinction ratio for blue and green wavelengths is ~1000 and for red wavelengths the extinction ratio is ~100. The extinction ratios for unpatterned PVA evaluated with red wavelength is ~100. The data in Figure 11 demonstrates that the polarization properties of the micro polarization PVA structures, created using selective RIE are not altered and they are similar to the polarization properties of an unpatterned and an un-etched PVA filter.
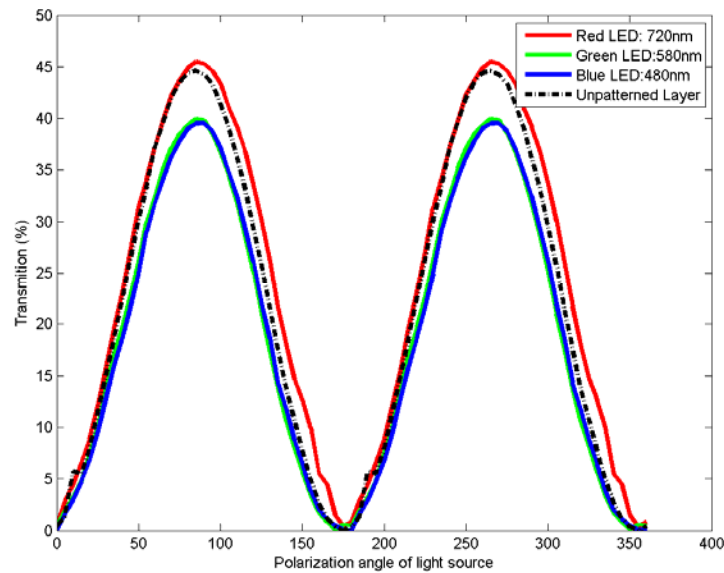

Figure 11: Transmission of a single PVA micro structure under different wavelengths. The transmission properties of unpatterned PVA are also presented.

6. Conclusion

An outline of a novel polarization filtering architecture for real time polarimetric imaging has been described. This sensory system requires accurate patterning of thin film polarizers. We have outlined the methodology necessary to pattern and etch 10μm-thick PVA polarizer in order to create 8μm by 8μm square structures. These methods would allow patterning of polarization micro structures necessary to be placed on top of an imaging sensor. The extinction ratios of the polarization filter are around 1000 for blue and green wavelength and 100 for red wavelengths. In our next phase of research efforts, the final array of micro polarizer will be mounted on top of a custom made image sensor for real time polarimetric computation.

7. Acknowledgment